1998

Effects of the Drake Passage on the global climatic change

Chu, Peter C.; Chen, Yunchun; Lu, Shihua

Chu, P.C., S.H. Lu, and Y. Chen, 1998: Effects of the Drake Passage on the global climatic change. Ninth Conference on Global Change, American Meteorological Society, 261-265
https://hdl.handle.net/10945/36235

EFFECTS OF DRAKE PASSAGE ON GLOBAL CLIMATE CHANGE

Peter C. Chu, Shihua Lu and Yuchun Chen
Department of Oceanography, Naval Postgraduate School, Monterey, CA 93943

1 INTRODUCTION

The Drake Passage cuts the connection between the South American and Antarctic continents. Along the entire length of the latitude circles where the Drake Passage extends, the water can travel around the earth forming a zonal flow - the Antarctic Circumpolar Current (ACC). This is the only place in World Ocean that the zonal flow can travel around the earth without land blocking. Thus, the Drake Passage has been considered an important factor in the global ocean circulation. Using a primitive equation model, Cox (1989) pointed out that if the Drake Passage closed, thermohaline drives alone and the entire World Ocean below the thermocline is dominated by water formed near the Antarctic continent. When the Drake Passage is opened, the resulting ACC serves to isolate the extreme Southern Ocean. Thus, the absence of the Drake Passage is to strengthen the thermohaline circulation.

Taking the atmosphere and oceans as a coupled system, strengthening of the thermohaline circulation leads to an increase in the pole-ward heat transport, causes the high latitude warming, and reduces the latitudinal gradient of surface temperature (SST). Such a reduction in SST gradient weakens the baroclinic instability in the atmosphere and changes the atmospheric general circulation. The change of the atmospheric circulation feeds back to oceans by varying surface fluxes of momentum, heat, and water mass. This air-ocean feedback mechanism has been discussed in simple models (Chu et al., 1990; Chu and Garwood, 1991). Here, we use a more sophisticated coupled atmosphere-ocean numerical model to investigate the effect of Drake Passage on global climate change by comparing two simulations: (1) control run (realistic bottom topography for the ocean model), and (b) anomaly run (Drake Passage closed for the ocean model).

2 COUPLED ATMOSPHERE-OCEAN MODEL

2.1 General Description

A coupled atmosphere-ocean model developed at the Institute for Space Studies at NASA/Goddard Space Flight Center (Russell, et al., 1995), called the GISS coupled model, was used for this study. The atmospheric model is similar to that of Hansen et al. (1983) except that the atmospheric dynamic equations for mass and momentum are solved using a stagged grid scheme and the advection of potential enthalpy and water vapor uses the linear upstream scheme (Russell and Lerner, 1981). The global ocean model conserves mass, allows for divergent flow, and has a free surface and uses the linear upstream scheme for the advection of potential enthalpy and salt. Both models run at $4°\times5°$ resolution, with 9 vertical layers and 13 layers for the ocean. Twelve straits are included, allowing for subgrid-scale water flow. Runoff from land is routed into approximate ocean basins. Atmospheric and oceanic surface fluxes of water, heat (excluding solar radiation), and momentum are of opposite sign and are applied synchronously. Flux adjustments are not used. Except for partial strength alternating binomial filters, which are applied to the momentum components in the atmosphere and oceans, there is no explicit horizontal diffusion. The solar irradiance is taken as 1367 W m^{-2}. For more information about this coupled model, readers are referred to Russell (1994) and Russell et al. (1995).

2.2 Sea-Ice Parametrization

When the energy losses cause the first layer of the open ocean to cool below the freezing point, the ocean stays at the freezing point and 0.5 m thick ice is formed. With additional energy loss the sea ice thickens, as seen in Hansen et al. (1988). Since the model assumes no salt in the sea ice, the salt concentration of the first ocean layer increases when sea ice forms or thickens. When surface fluxes, principally insolation, case the sea ice temperature to rise above 0°C and snow or sea ice melts, which joins the ocean below. If sea ice becomes thinner than

0.5 m, then it is contracted horizontally so that it remains 0.5 m thick. If the temperature of the first ocean layer rises above 0°C, then sea ice is melted vertically and horizontally, drawing the necessary energy from the ocean which cools back to 0°C. The temperature within the sea ice is determined by a two-layer model. Leads in the sea ice are calculated as was done by Hansen et al. (1984): the minimum fraction of open ocean in a grid box is $0.1h_i^{-1}$, where h_i is the sea ice thickness in meter.

2.3 Land Albedo

Land albedo is a function of vegetation type including seasonal variations and separate albedos for the visible and near infrared regions.

2.4 Ocean Albedo

The ocean albedo is a specific function of surface wind speed (V_s) and solar zenith angle (θ):

$$\begin{aligned}\alpha_w = & \ 0.012 + 0.0421x^2 + 0.1283x^3 \\ & -0.04x^4 + \tfrac{3.12x^5}{5.68+V_s} + \tfrac{0.074x^6}{1+3V_s}\end{aligned} \qquad (1)$$

where $x = 1 - \cos^{-1}\theta_0$. This parameterization is based on calculations of Fresnel reflection from the ocean surface as a function of V_s as specified by Cox and Munk (1956).

2.5 Ice Albedo

The ice albedo, α_i, is treated as wavelength dependent:

$$\alpha_i = \begin{matrix} 0.55 & \text{visible} \\ 0.3 & \text{near infrared} \end{matrix} \qquad (2)$$

where the visible is defined as wavelengths $< 0.7\ \mu m$, corresponding to 60% of solar irradiance. Such a treatment leads to a spectrally weighted ocean albedo of 0.45.

3 EXPERIMENTAL DESIGN

3.1 Control Run

The initial condition used in this study is obtained from the National Centers for Environmental Prediction (NCEP) atmospheric observations for 1 July 1990, and from the National Ocean Data Center (NODC) global climatological mean July temperature and salinity fields at 1°×1° resolution. The time step is 7.5 minutes. We integrated the GISS coupled model for 66 months.

3.2 Anomaly Run

After six months of the control run, we replaced the bottom topography with the Drake Passage closed. The rest of the forcing was kept unchanged. The model were integrated for another 60 months. Total integration period is 66 months. We compare the air-ocean variables between the two runs for the monthly averaged data between 3rd to 5th year (equivalent to **January-December**).

3.3 Effect of the Drake Passage Closed

The effect of the Drake Passage closed is represented by the difference of the two runs (anomaly run minus control run) of any surface variable ψ,

$$\Delta\psi(x_i, y_j, t) = \psi_a(x_i, y_j, t) - \psi_c(x_i, y_j, t).$$

which is called the ψ **difference** in this study. Here, ψ_a and ψ_c are the variables from anomaly and control runs, respectively. We use the last two years' data for comparison.

4 GLOBAL CLIMATE CHANGE CAUSED BY THE DRAKE PASSAGE CLOSURE

The Drake Passage closure causes severe global change, such as strengthening thermohaline circulation, increasing the Indonesia Through-Flow, weakening the ACC, causing high latitude warming (especially the Antarctic), reducing of latitudinal sea surface temperature (SST) gradient, and weakening the atmospheric activities.

4.1 Ocean Circulation

Difference (anomaly run minus control run) in the surface layer (0-150 m) mass transport (Fig.1) shows drastic change in the equatorial and Southern Hemisphere ocean circulation such as in the ACC, equatorial currents, the western boundary currents, and the Indonesia Through Flow. However, it shows no evident effect on the ocean circulation north to 30°N.

The closure of the Drake Passage blocks the zonal flow and weakens the Antarctic Circumpolar Current in both winter (Fig.1a) and summer (Fig.1b) and leads to the formation of several eddies near the Antarctic Continent. The radius of the eddies is around 500 km. An evident cyclonic-anticyclonic dipole appears in the Indian Ocean section between 45°S and the Antarctic Continent.

The closure of the Drake Passage affects the Southern Hemisphere western boundary currents such as a 15-Sv increase in the Brazil Current, a 4-Sv decrease in the Somali Current, and a 5-Sv increase in the Eastern Australian Coastal Current. Furthermore, it enhances the equatorial currents (especially the southern equatorial current) and the Indonesia Through Flow (5-Sv increase).

4.2 Latitudinal Oceanic Heat Transport

The Drake Passage closure enhances the thermohaline circulation, which in turn changes the latitudinal heat transport. Taking the Atlantic Ocean as an example, the northward heat transport is greatly reduced when the Drake Passage is closed (Fig.2). The heat is usually transported from low latitudes to high latitudes. Thus, the Drake Passage closure strengthens (slightly weakens) the pole-ward heat transport in the Northern (Southern) Hemisphere. This leads to reductions in both latitudinal SST gradient and sea ice concentration (especially in the Southern Hemisphere).

4.3 Latitudinal SST Gradient Reduction

The change of the heat transport causes the reduction of latitudinal SST gradient (Fig.3). Obvious warming appears in the polar regions especially near the Antarctic Continent ($\Delta SST > 4°C$). In the mid-latitudes (20°N-45°N, 30°S-45°S), ΔSST is generally negative with a maximum reduction of 1.4°C. Polar warming/mid-latitude cooling leads to a weakening of the latitudinal SST gradient.

4.4 Sea-Ice Reduction

The polar warming causes the sea-ice reduction especially in the Antarctic regions (Fig.4). Obvious sea-ice reduction appears near the Antarctic Continent in both seasons.

4.5 Atmospheric Surface Winds

The attenuation of the latitudinal SST gradient reduces the baroclinicity, which in turn weakens the strength of atmospheric circulation. This can be identified by the global surface wind vector differences (Fig.5). The Aleutian Low, Polar Low near the GIN Sea, and the Subtropical High over the North Atlantic Ocean are greatly reduced in January (Fig.5a). However, the Subtropical Highs over both Pacific Ocean and Atlantic Ocean are weakened in July (Fig.5b). Thus, the Drake Passage closure leads to a **weakening of the atmospheric general circulation.**

5 CONCLUSIONS

The effect of the Drake Passage closure on the global climate change has been identified by the GISS air-sea coupled model. Our results show that the closure of the Drake Passage causes a drastic enhancement in the equatorial currents, in the thermohaline circulation and the western boundary currents especially in the Southern Hemisphere, and in turn increases the pole-ward heat transport in the Southern Hemisphere middle and high latitudes. Thus, it reduces the latitudinal thermal inhomogeneity. The weakening SST latitudinal gradient reduces the atmospheric baroclinicity and in turn reduces the atmospheric activities such as weakening of the Aleutian Low, Polar Low near the GIN Sea, and the Subtropical High over the North Atlantic Ocean in winter and of the Subtropical Highs over both Pacific Ocean and Atlantic Ocean are weakened in summer.

6 ACKNOWLEDGMENTS

Authors are indebted to Gary L. Russell at NASA Goddard Institute for Space Studies for allowing us to use the coupled atmosphere-ocean model. This work was funded by the Office of Naval Research NOMP Program, and the Naval Postgraduate School.

References

Chu, P.C., R.W. Garwood, Jr., and P. Muller, 1990: Unstable and damped modes in coupled ocean mixed layer and cloud models. *J. Mar. Syst.*, **1**, 1-11.

Chu, P.C., and R.W. Garwood, Jr., 1991: On the two-phase thermodynamics of the coupled cloud-ocean mixed layer. *J. Geophys. Res.*, **96**, 3425-3436.

Cox, M., 1989: An idealized model of the world ocean. Part I: the global scale water masses. *J. Phys. Oceanogr.* **19**, 1730-1752.

Hansen, J., G. Russell, D. Rind, P. Stone, A. Lacis, S. Lebedeff, R. Ruedy, and L. Travis, 1983: Efficient three-dimensional global models for climatic studies: Model I and II. *Mon. Wea. Rew.*, **111**, 609-662.

Russell, G.L., J.R. Miller, and D. Rind, 1995: A coupled atmosphere-ocean model for transient climate change studies. *Atmosphere-Ocean*, **33**, 683-730.

Russell, G.L., and J.A. Lerner, 1981: A new finite-differencing scheme for the tracer transport equation. *J. Appl. Meteorol.*, **20**, 1483-1498.

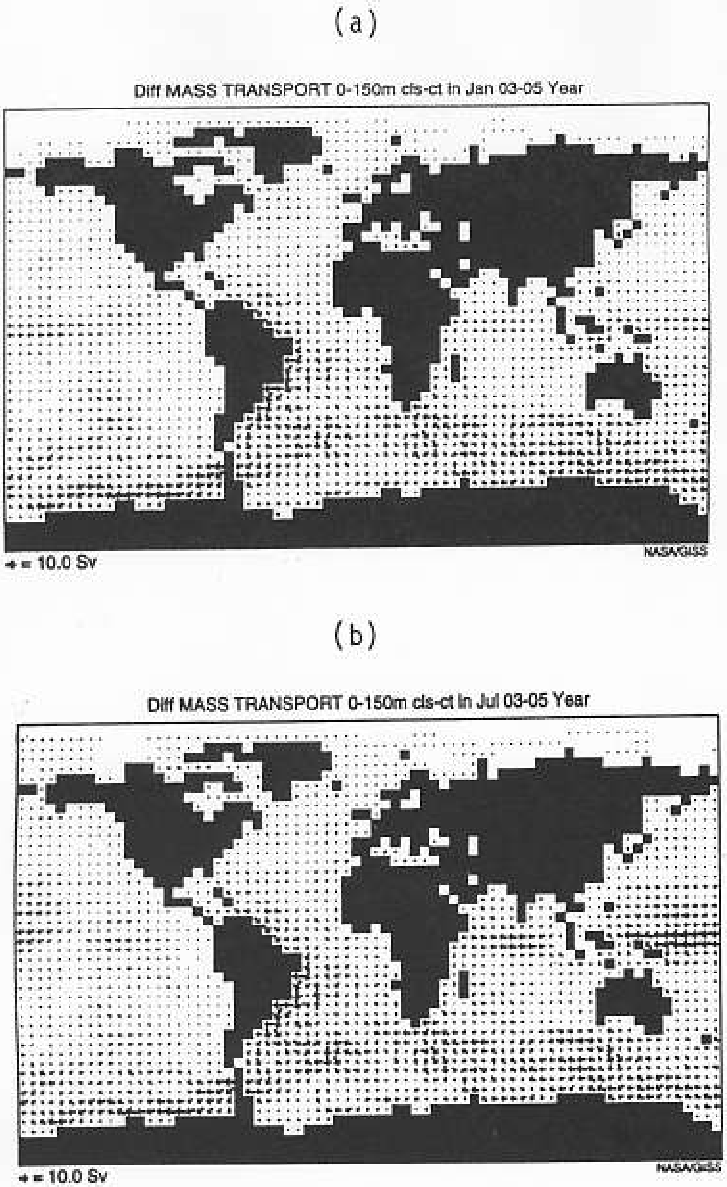

Figure 1 – Surface layer (0 - 150 m) mass transport difference (Sv) from anomaly run minus control run: (a) January, and (b) July.

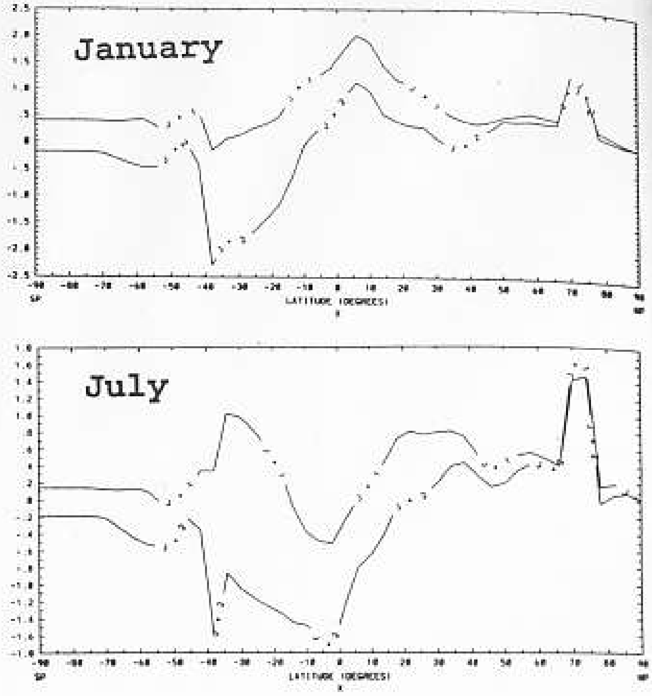

Figure 2 – Northward heat transport in the Atlantic Ocean for (a) January, and (b) July. Here the curve 1 indicates the control run and the curve 2 means the anomaly run.

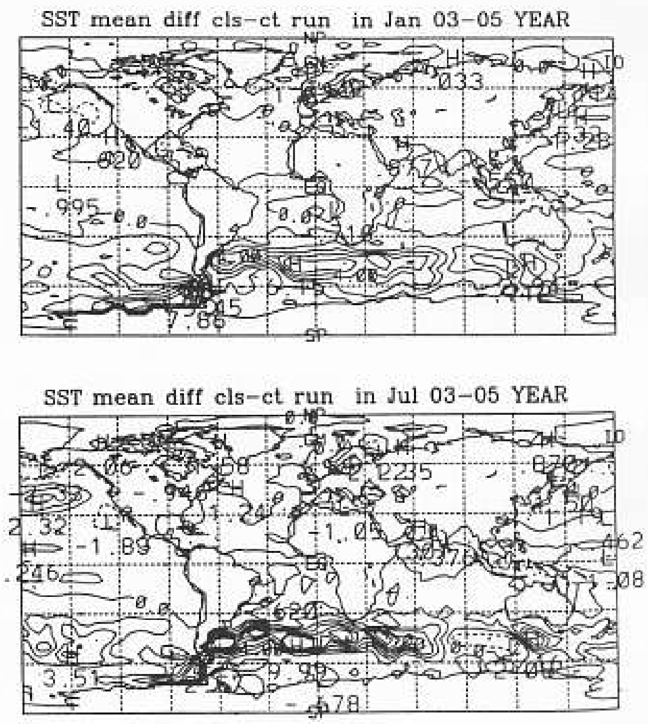

Figure 3 – SST difference for (a) January, and (b) July.

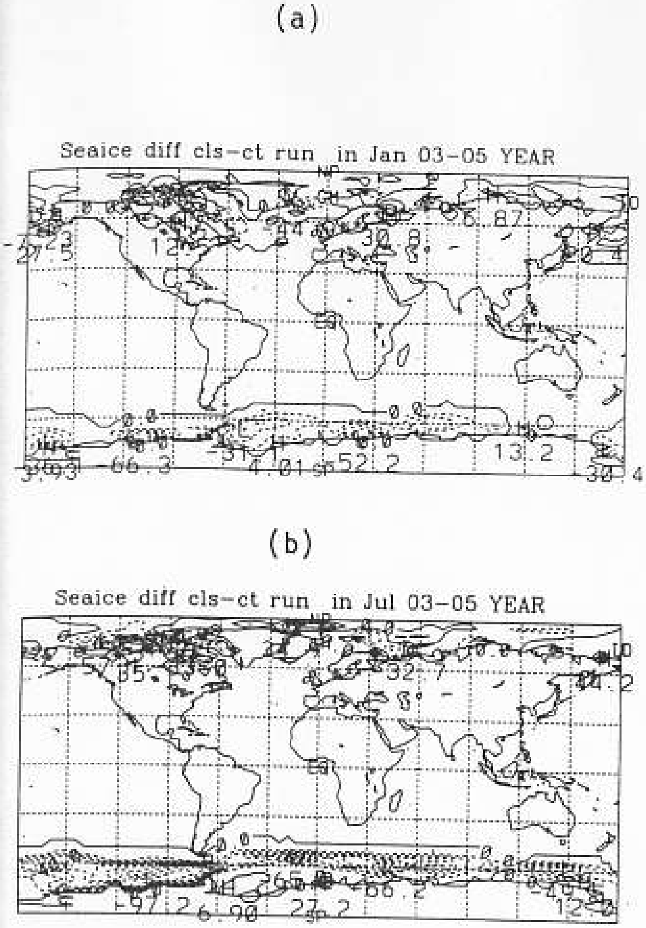

Figure 4 – Ice concentration difference: (a) January, and (b) July.

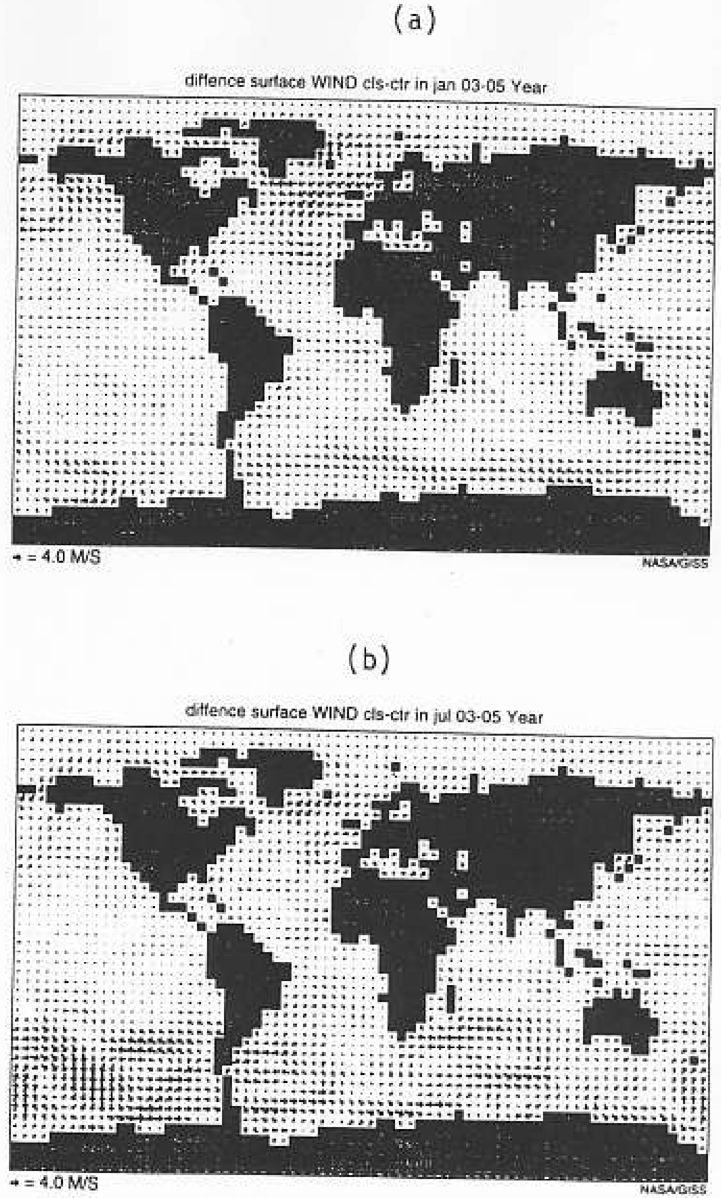

Figure 5 – Surface wind vector difference: (a) January, and (b) July.